Multidisciplinary | Rapid Review | Open Access Journal

Received December 8, 2020, accepted December 23, 2020, date of publication January 8, 2021, date of current version January 19, 2021.

Digital Object Identifier 10.1109/ACCESS.2021.3049770

On the Cooperative Relaying Strategies for Multi-Core Wireless Network-on-Chip

QUOC-TUAN VIEN[1], (Senior Member, IEEE), MICHAEL OPOKU AGYEMAN[2], (Senior Member, IEEE), MALLIK TATIPAMULA[3], (Senior Member, IEEE), AND HUAN X. NGUYEN[1], (Senior Member, IEEE)

[1]Faculty of Science and Technology, Middlesex University, London NW4 4BT, U.K.
[2]Department of Computing and Immersive Technologies, University of Northampton, Northampton NN1 5PH, U.K.
[3]Ericsson Silicon Valley, Santa Clara, CA 95054, USA

Corresponding author: Quoc-Tuan Vien (q.vien@mdx.ac.uk)

This work was supported in part by a UKIERI grant, ID 'DST UKIERI-2018-19-011', and in part by an Institutional Links grant, ID 429715093, under the Newton Programme Vietnam partnership. The grants are funded by the UK Department for Business, Energy and Industrial Strategy and DST (India) and delivered by the British Council (https://www.newton-gcrf.org).

ABSTRACT Recently, hybrid wired-wireless Network-on-Chip (WiNoC) has been proposed as a suitable communication fabric to provide scalability and satisfy high performance demands of the exascale era of modern multi/many-core System-on-Chip (SoC) design. A well accepted low-latency wireless communication fabric for WiNoCs is millimeter wave (mm-Wave). However, the wireless channel of mm-Wave is lossy due to free space signal radiation with both dielectric propagation loss (DPL) and molecular absorption attenuation (MAA). This is exacerbated for edge situated cores and in macro-chips embodying thousands of cores. To this end, this article proposes efficient relaying techniques to improve the signal strength of the wireless channel in the WiNoCs using on-chip networking approaches under the realistic SoC channel conditions. First, we propose a realistic relay communication channel for the WiNoCs to characterise both MAA and DPL which have drastic effect on the performance. We then derive and show that the channel capacity for a single-relay WiNoC employing Amplify-and-Forward (AF) and Decode-and-Forward (DF) relaying protocols increases by up to 20% and 25%, respectively, compared to the conventional direct transmission. The AF protocol outperforms the DF mode for shorter transmissions between the relay and the destination cores, while the reverse is observed in other conditions. A hybrid protocol is then proposed to exploit the performance advantages of both relaying protocols to address the unbalanced distance between the cores, providing the maximal channel capacity close to the cutset bound. Finally, our approach is further validated in multi-relay WiNoCs where the communications of the remote cores is assisted by multiple intermediate cores along with the details of associated realistic channel model in emerging many-core SoCs.

INDEX TERMS Channel modeling, cooperative diversity, relay networks, wireless network-on-chip, WiNoC.

I. INTRODUCTION

With growing and emerging multimedia applications which require a considerable enhancement of computation and interactive functionality, wire-based interconnects between cores in a Network-on-Chip (NoC) have been shown to be insufficient to meet the critical requirements of high performance, scalability and low latency, especially in this technological era of ever increasing number of cores [1], [2]. In order to address these issues, various alternative fabrics and architectures for NoCs have been investigated, such as photonic NoC [3], [4], nanophotonic NoC [5], three-dimensional NoC (3D NoC) [6]–[8] and Wireless NoC (WiNoC) [9]–[13]. Specifically, the WiNoC with its flexibility and scalability over the wireless medium is shown to considerably reduce the propagation delay of intra-chip communications. By exploiting the high frequency band of up to terahertz [14], a massive number of wireless cores can be accommodated in a limited area of WiNoC.

Although WiNoC is well known in literature as a promising approach to replace the conventional NoCs, an appropriate channel modelling is required to realise the impacts of the propagation environment when transmitting electromagnetic waves at high frequency [15]. The wireless medium within the chip is shown to have considerable impacts on the communications between the wireless cores in the WiNoC [12]. The operating temperature, ambient pressure and compositions of the wireless medium are all reflected in the channel

The associate editor coordinating the review of this manuscript and approving it for publication was Xiwang Dong.

capacity of the WiNoC. In particular, a small increase of the distance between the cores cause a far lower performance due to the existence of both propagation loss and molecular absorption, and hence may limit its application for a number of cores, some of which are located far from each other [12].

Inspired by the relaying concept in wireless network with user cooperation [16], [17], in this article, we investigate the employment of relaying techniques to enhance the communications on a chip. The communication between the far end wireless cores is assisted by intermediate cores which play the role as relays in the wireless network. The intermediate cores can employ either amplify-and-forward (AF) or decode-and-forward (DF) relaying protocols. In the DF protocol, the relay core decodes the signal from the source core prior to transmitting to the destination core, while the relay employing AF protocol simply amplifies the signal from the source core and forward it to the destination core. It was shown in [16] that the DF protocol depends on the quality of the first hop, and thus its diversity is limited to one in the worst case when the relay cannot decode the signal from the source. Instead, a full diversity can be achieved with the AF protocol when the destination receives different versions of the signal from the source and relay; however, the relay in this protocol also amplifies and forwards the noises together with the signals to the destination. Although these two relaying techniques have been well developed in the literature for wireless networks, their employment in the WiNoC, to the best of the authors' knowledge, has not been investigated.

To this end, the contributions of the work in this article can be summarised as follows:

- A relay communication channel is proposed for the communications between wireless cores in a WiNoC taking into account the dielectric material and compositions of the transmission medium within the chip package, such as water vapour, oxygen, carbon dioxide, etc. Such mixture of material substance at high frequency causes not only dielectric propagation loss (DPL), but also molecular absorption attenuation (MAA) of the electromagnetic wave travelling between the cores, which consequently have considerable impacts on the performance of the WiNoC.
- The channel capacity is derived for a typical single-relay WiNoC where all links experience both DPL and MAA. Two relaying protocols, i.e. DF and AF, are sequentially considered at the intermediate core to assist the communications between two end cores. The impacts of the channel model on the performance of the relaying in the WiNoC are firstly evaluated, showing that not only the distance between the cores as in the conventional wireless channels but also the ambient pressure and system electronic noise temperature cause considerable degradation of the capacity of the relaying channels. It is shown that the channel capacity of both protocols is higher than that of the DT, while they are upper bounded by the cutset bound of the relay channel. In addition, the physical distance between the cores is shown to have considerable impacts on the performance. Specifically, the AF outperforms the DF protocol when the intermediate core is located near the destination core, otherwise the DF is preferable with a better performance.
- A hybrid DF-AF (HDA) relaying protocol is proposed, where an intermediate core can perform either DF or AF relaying depending on its position with respect to two end cores. The proposed protocol is shown to achieve the best performance over both the DF and AF protocols regardless of the location of the intermediate core.
- The proposed HDA protocol is extended for a multi-relay WiNoC where the communications between two end cores is realised with the assistance of multiple intermediate cores. In the proposed protocol, maximum ratio combining (MRC) is employed at the destination core to combine the data received from not only direct link but also relaying links. The channel capacity of the HDA protocol is derived for the multi-relay channel and validated through numerical results.

The rest of this article is organised as follows: Section II reviews the related works on the employment of wireless cores in WiNoCs. Section III describes the system model of a multi-core WiNoC with the introduction of relay communication channels between the wireless cores. A typical channel for the conventional point-to-point communications in the WiNoC is discussed in Section IV, followed by the analysis of its channel capacity in Section V. Section VI derives the capacity of a typical relay channel in the WiNoC where the intermediate core employs either DF or AF relaying protocols. The proposed HDA protocol is developed in Section VII for a multi-relay WiNoC. Numerical results are presented in Section VIII to validate the performance of the relay communications in the WiNoC and the proposed HDA protocol. Section IX finally draws the main contributions from this article.

II. RELATED WORKS

Recent technological advances makes it feasible to integrate wireless transceivers on a silicon die [18]. Consequently, various contributions have been made in literature to improve the power and performance efficiency of traditional wire-based NoCs by augmenting long ranged wireless channels in the form of mm-wave forming hybrid architectures [19], [20]. Hybrid WiNoCs which benefit from both the high throughput and power efficiency of both localized and low latency global data transmission have extensively been studied in literature [12], [21], [22]. One of the main challenges with WiNoCs is that wireless channel is lossy and has high signal-to-noise ratio [12]. In attempt to resolve the aforementioned issue, Deb *et al.* [9] proposed an error-control-coding for WiNoCs. Their work demonstrates that implementing WiNoCs with joint crosstalk triple error correction and simultaneous quadruple error detection codes in the wire line links and Hamming code based product codes in the wireless links with Carbon Nanotube (CNT) antennas, improves the reliability of the wireless channel.

Similarly, ECC and error Control Units have been employed in [9] and [23], respectively, to improve the reliability of WiNoCs. However, ECC introduces timing, area and packet overheads which affects the overall transmission efficiency of the WiNoC [24]. Alternatively, Lee *et al.* [24] adopted an overhearing scheme for WiNoCs. Here, a zero-signaling-overhearing-and-retransmission is presented to manage the packet loss along the wireless channel. A checksum-based error-detection and retransmission scheme at the last hop. Vijayakumaran *et al.* [25] proposed an improved filter design to improve the performance and reduce the error probability incurred by synchronization delays in CDMA based WiNoCs. However, the underlying lossy wireless communication fabric results in retransmission of handshake signals, erroneous packets, especially for global wireless transmissions involving remotely situated cores.

Inspired by the relaying concept in wireless network with user cooperation [17], in this article, we investigate the employment of cooperative networking techniques to tackle the issue of poor signal strength of global data transmission along the wireless channel in WiNoCs. The intermediate core can assist the communications between remote cores using either DF or AF relaying protocols. In [26], a utility maximization framework was proposed to jointly find the best relay node with opportunistic relay strategy selection and the best power and bandwidth allocations in cellular networks. The optimal power allocation for DF and AF protocols was also derived in [27] for Rayleigh fading channels. Our aim in this work is to optimize the communication along the wireless channel for remote cores in WiNoCs to compliment existing high performance wireless communication fabrics in order to improve the reliability of the wireless interface of WiNoCs.

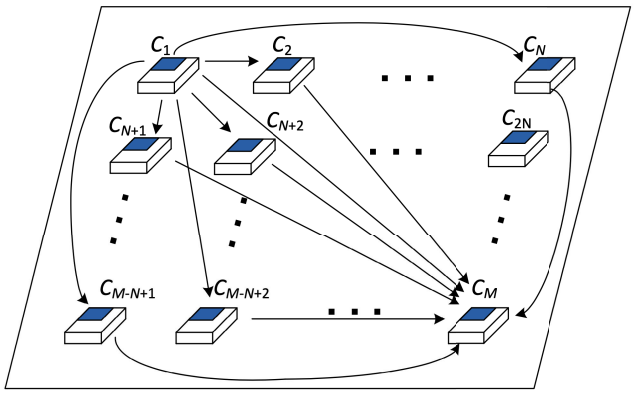

FIGURE 1. System model of a multi-core WiNoC package.

III. SYSTEM MODEL OF A WINOC

The system model of a WiNoC under investigation is illustrated in Fig. 1 where M cores are allocated as in a two-dimensional grid graph. The transmission between two wireless cores $\mathcal{C}_s$ and $\mathcal{C}_d$, $\{s, d\} \in \{1, 2, \ldots, M\}$, $s \neq d$, can be realised with the assistance of intermediate wireless cores $\{\mathcal{C}_{r_i}\}$, $r_i \in \{1, 2, \ldots, M\} \setminus \{s, d\}$. It is assumed that each core is equipped with a single antenna and a half-duplex system is considered where each core can either send or receive data, but not simultaneously. Let h_i and d_{ij}, $\{i, j\} \in \{1, 2, \ldots, M\}$, $i \neq j$, denote the height of the antenna at $\mathcal{C}_i$ and the distance between $\mathcal{C}_i$ and $\mathcal{C}_j$, respectively.

The wireless communication between two cores is performed at frequency f [Hz] with an allocated channel bandwidth of B [Hz] and the material property of the transmission medium within the chip package is represented by the relative permittivity (or dielectric constant) $\epsilon_r \geq 1$ [28]. The compositions of the transmission medium, including water vapour, oxygen, carbon dioxide, etc., are assumed to be time-invariant over the transmission of a data frame. It is assumed that there are N gases $\{\mathcal{G}_1, \mathcal{G}_2, \ldots, \mathcal{G}_N\}$ in the chip package, each of which has N_g, $g = 1, 2, \ldots, N$, isotopologues $\{\mathcal{I}_{g,1}, \mathcal{I}_{g,2}, \ldots, \mathcal{I}_{g,N_g}\}$. The signal transmission between two wireless cores in the WiNoC suffers both DPL and MAA which is caused by dielectric material, molecules and their isotopologues [12].

IV. CHANNEL MODEL FOR POINT-TO-POINT COMMUNICATIONS IN A WINOC

In this section, let us consider a wireless point-to-point (P2P) communication link between two cores $\mathcal{C}_i$ and $\mathcal{C}_j$, $\{i, j\} \in \{1, 2, \ldots, M\}$, $i \neq j$, in a relay channel. The total attenuation of electromagnetic signal transmitted from $\mathcal{C}_i$ to $\mathcal{C}_j$ consists of DPL and MAA as follows:[1]

1) DIELECTRIC PROPAGATION LOSS (DPL)

Let $P_{T,i}$ [W], $P_{R,j}$ [W], $G_{T,i}$ and $G_{R,j}$, $\{i, j\} \in \{1, 2, \ldots, M\}$, $i \neq j$, denote the transmitted power at $\mathcal{C}_i$, received power at $\mathcal{C}_j$, transmitting antenna gain at $\mathcal{C}_i$ and receiving antenna gain at $\mathcal{C}_j$, respectively. The received power at $\mathcal{C}_j$ can be computed by [29]

$$P_{R,j} = \frac{P_{T,i} G_{T,i} G_{R,j}}{\left(\frac{2\pi d_{ij} f}{v_p}\right)^2} \sin^2\left(\frac{2\pi h_i h_j f}{v_p d_{ij}}\right), \tag{1}$$

where v_p [m/s] denotes the phase velocity in the dielectric given by $v_p = c/\sqrt{\epsilon_r}$ [28] and $c = 2.9979 \times 10^8$ m/s is the speed of light in the vacuum.[2]

Letting $L_{ij}^{(d)}$ denote the DPL of the link $\mathcal{C}_i \to \mathcal{C}_j$, we then have

$$L_{ij}^{(d)} = \frac{P_{T,i}}{P_{R,j}} = \left(\frac{2\pi d_{ij} f}{c}\right)^2 \frac{\epsilon_r}{G_{T,i} G_{R,j}} \csc^2\left(\frac{2\pi h_i h_j f \sqrt{\epsilon_r}}{c d_{ij}}\right). \tag{2}$$

2) MOLECULAR ABSORPTION ATTENUATION (MAA)

The electromagnetic wave travelling from core $\mathcal{C}_i$ to core $\mathcal{C}_j$, $\{i, j\} \in \{1, 2, \ldots, M\}$, $i \neq j$ is subjected to MAA caused by

[1] While full details with derived expressions for P2P communications can be referred to in our preliminary work in [12], a brief introduction is provided here for completeness of our derived channel model for relay communications in the WiNoC.

[2] Note that, different from the wireless communications over the free space with $v_p = c$, i.e. $\epsilon_r = 1$, the communication between two cores in a WiNoC is affected by the relative permittivity of the material within the chip, e.g. $\epsilon_r = 3.9$ for silicon dioxide and $\epsilon_r = 11.9$ for silicon [30]

N molecules (or gases) $\{\mathcal{G}_1, \mathcal{G}_2, \ldots, \mathcal{G}_N\}$ within the material substance, each of which includes N_g, $g = 1, 2, \ldots, N$, isotopologues $\{\mathcal{I}_{g,1}, \mathcal{I}_{g,2}, \ldots, \mathcal{I}_{g,N_g}\}$ [31]. Following the same approach as in [12], the MAA of the link $\mathcal{C}_i \rightarrow \mathcal{C}_j$, denoted by $L_{ij}^{(a)}$, can be determined by applying Beer-Lambert's law as

$$L_{ij}^{(a)} = \frac{1}{\tau_{ij}} = e^{\kappa d_{ij}}, \tag{3}$$

where τ_{ij} and κ [m^{-1}] denote the transmittance of the medium between $\mathcal{C}_i$ and $\mathcal{C}_j$ and the medium absorption coefficient, respectively. Here, κ can be determined by applying radiative transfer theory [32] to each of the $\{k_g\}$ isotopologues of the $\{g\}$ gases, $g = 1, 2, \ldots, N$, $k_g = 1, 2, \ldots, N_g$, as follows:[3]

$$\kappa = \frac{\zeta_A}{\zeta_G}\frac{p^2}{p_0}\frac{T_p}{T_S^2}\sum_{g=1}^{N}\sum_{k_g=1}^{N_g} q^{(k_g,g)} S^{(k_g,g)} \xi^{(k_g,g)}, \tag{4}$$

where p [atm], T_S [K], $q^{(k_g,g)}$ [%], $S^{(k_g,g)}$ [m^2Hz/mol] and $\xi^{(k_g,g)}$ [Hz^{-1}] denote the ambient pressure applied on the chip, the system electronic noise temperature, the mixing ratio, the line density of the absorption and the spectral line shape of (k_g, g), respectively.[4] In (4), $p_0 = 1$ atm, $T_p = 273.15$ K, $\zeta_G = 8.2051 * 10^{-5}$ m^3atm/K/mol and $\zeta_A = 6.0221 * 10^{23}$ mol^{-1} denote the reference pressure, the temperature at standard pressure, the Gas constant and the Avogadro constant, respectively. The spectral line shape $\xi^{(k_g,g)}$ is given by

$$\xi^{(k_g,g)} = \frac{f}{f_c^{(k_g,g)}} \frac{\tanh\left(\frac{\zeta_P v_p f}{2\zeta_B T_S}\right)}{\tanh\left(\frac{\zeta_P f_c^{(k_g,g)}}{2\zeta_B T_S}\right)} \upsilon^{(k_g,g)}, \tag{5}$$

where $\zeta_P = 6.6262 * 10^{-34}$ Js, $\zeta_B = 1.3806 * 10^{-23}$ J/K, $f_c^{(k_g,g)}$ [Hz] and $\upsilon^{(k_g,g)}$ [Hz^{-1}] denote the Planck constant, the Boltzmann constant, the resonant frequency and the Van Vleck-Weisskopf asymmetric line shape of (k_g, g), respectively. Here, $f_c^{(k_g,g)}$ and $\upsilon^{(k_g,g)}$ can be determined by

$$f_c^{(k_g,g)} = f_{c_0}^{(k_g,g)} + \delta^{(k_g,g)}\frac{p}{p_0}, \tag{6}$$

$$\upsilon^{(k_g,g)} = 100 v_p \frac{\alpha_L^{(k_g,g)}}{\pi}\frac{f}{f_c^{(k_g,g)}}\left[\frac{1}{(f - f_c^{(k_g,g)})^2 + (\alpha_L^{(k_g,g)})^2} + \frac{1}{(f + f_c^{(k_g,g)})^2 + (\alpha_L^{(k_g,g)})^2}\right], \tag{7}$$

respectively, where $f_{c_0}^{(k_g,g)}$ [Hz], $\delta^{(k_g,g)}$ [Hz] and $\alpha_L^{(k_g,g)}$ [Hz] denote the resonant frequency of (k_g, g) at reference pressure $p_0 = 1$ atm, the linear pressure shift and the Lorentz half-width of (k_g, g), respectively. In (7), $\alpha_L^{(k_g,g)}$ is computed by

$$\alpha_L^{(k_g,g)} = \left[(1 - q^{(k_g,g)})\alpha_0 + q^{(k_g,g)}\beta^{(k_g,g)}\right]\frac{p}{p_0}\left(\frac{T_0}{T_S}\right)^{\omega}, \tag{8}$$

[3]For simplicity, the k_g-th isotopologue of the g-th gas is hereafter denoted by (k_g, g), unless otherwise stated.

[4]Note that $q^{(k_g,g)}$ [%] and $S^{(k_g,g)}$ can be obtained from high-resolution transmission (HITRAN) molecular absorption database [31].

where $T_0 = 296$ K, α_0 [Hz], $\beta^{(k_g,g)}$ [Hz] and ω denote the reference temperature, the broadening coefficient of air, the broadening coefficient of (k_g, g) and the temperature broadening coefficient, respectively.

3) TOTAL ATTENUATION IN THE PROPOSED CHANNEL MODEL

Taking into consideration both DPL and MAA, let us denote by L_{ij}, $\{i, j\} \in \{1, 2, 3\}$, $i \neq j$, the total attenuation of the signal transmission from $\mathcal{C}_\rangle$ to $\mathcal{C}_|$. From (2), (3) and (4), L_{ij} can be expressed as

$$L_{ij} = L_{ij}^{(d)} L_{ij}^{(a)} = \left(\frac{2\pi d_{ij} f}{c}\right)^2 \frac{\epsilon_r}{G_i G_j} \csc^2\left(\frac{2\pi h_i h_j f\sqrt{\epsilon_r}}{c d_{ij}}\right) \times \prod_{g=1}^{N}\prod_{k_g=1}^{N_g} e^{\frac{\zeta_A}{\zeta_G}\frac{p^2}{p_0}\frac{T_p}{T_S^2} q^{(k_g,g)} S^{(k_g,g)} \xi^{(k_g,g)} d_{ij}}. \tag{9}$$

It can be seen in (9) that all the physical parameters of the antennas deployed on two wireless cores, such as antenna gain (i.e. $G_{T,i}$, $G_{R,j}$), height (i.e. h_i, h_j), frequency (i.e. f), the distance between them (i.e. d_{ij}), the chip material and the compositions of the transmission medium all constitute the attenuation between the two wireless cores. We have the following remarks:

Remark 1: It can be seen in (9) that L_{ij} varies as a function of the relative permittivity of the chip material (i.e. ϵ_r). In fact, when $\epsilon_r \rightarrow \infty$, we can deduce $L_{ij} \rightarrow \infty$ which means that all the data will be lost in a high permittivity medium. This accordingly reflects the significant impact of the chip material on the performance of the wireless communications within a chip package.

Remark 2: In (4), $\kappa \geq 0$ $\forall g = 1, 2, \ldots, N$ and $k_g = 1, 2, \ldots, N_g$, and thus it can be deduced $L_{ij}^{(a)} \geq 1$ (see (3)). This means, the MAA in addition to the DPL constitute the total attenuation in the WiNoC, while the conventional channel model is generally assumed over the pure air with no MAA.

Remark 3: The gas composition, the dielectric material, the system temperature T_S and the ambient pressure p all are involved in the channel modelling. Specifically, as shown in (9), L_{ij} monotonically decreases over T_S, but it exponentially increases over p.

In summary, the wireless medium within the chip package has a considerable impact on the P2P communications between two wireless cores in WiNoC, which will be reflected in the analysis of the capacity of the P2P communications and the relay communications of a general WiNoC in the following sections.

V. CAPACITY OF POINT-TO-POINT CHANNELS IN A WINOC

Prior to analysing the performance of relaying in WiNoC, this section first derives the capacity of the P2P communications between two wireless on-chip cores in WiNoC. It is assumed that the communication between two cores suffers

from additive white Gaussian noise.[5] At high frequency, e.g. mm-wave, the channel is highly frequency-selective, and thus the channel bandwidth can be divided into multiple narrow sub-bands which can be regarded as parallel channels. The capacity of the P2P channel in the WiNoC can be derived as follows:

Theorem 1: The capacity, in bits/s, of a Gaussian P2P channel between two wireless on-chip cores $\mathcal{C}_i$ and $\mathcal{C}_j$, $\{i, j\} \in \{1, 2, \ldots, M\}$, $i \neq j$, is determined by

$$C_{ij} = \max_{\substack{P_{T,i_1}, P_{T,i_2}, \ldots, P_{T,i_K} \\ \sum_{k=1}^{K} P_{T,i_k} = P_{T,i}}} \sum_{k=1}^{K} \Delta f \log_2\left(1 + P_{T,i_k} \Lambda_{ij,k}^2\right), \quad (10)$$

where Δf [Hz], P_{T,i_k} [W] and $\Lambda_{ij,k}$ denote the width of each sub-band, the transmission power at the k-th sub-band and the channel gain at f_k, respectively. Here, $\Lambda_{ij,k}$ captures the path loss and receiver noise of the wireless link $\mathcal{C}_i \rightarrow \mathcal{C}_j$, which is given by (11) *(see the bottom of the page).*

Proof: See Appendix A. □

In Theorem 1, it is crucial to find the optimal power allocated at sub-bands (i.e. $\{P_{T,i_k}\}$) so as to maximise the capacity of the P2P channel subject to limited total power available at the cores (i.e. $\sum_{k=1}^{K} P_{T,i_k} = P_{T,i}$, $i = 1, 2, 3$). We have the following proposition:

Proposition 1: The channel capacity of the point-to-point communications between two on-chip wireless cores $\mathcal{C}_i$ and $\mathcal{C}_j$, $\{i, j\} \in \{1, 2, \ldots, M\}$, $i \neq j$, in WiNoC can be obtained as

$$C_{ij} = \sum_{k=1}^{K} \Delta f \left(\log_2 \frac{\vartheta_{ij}}{\Psi_{ij,k}}\right)^+, \quad (12)$$

where $(x)^+ \triangleq \max\{0, x\}$, $\Psi_{ij,k} \triangleq \frac{1}{\Lambda_{ij,k}^2}$ and ϑ_{ij} can be found by water-filling method such that

$$\sum_{k=1}^{K} \left(\vartheta_{ij} - \Psi_{ij,k}\right)^+ = P_{T,i}. \quad (13)$$

Proof: The proof follows the same approach for power allocation in Gaussian parallel channels. For completeness, it is provided in Appendix B taking into account the channel variants in the WiNoC context. □

Notice that the antenna size is much smaller than the distance between two wireless cores in a WiNoC. The channel capacity of the P2P channel can be approximated by

Corollary 1: When $h_i \ll d_{ij}$, $h_j \ll d_{ij}$, $d_{ij} \rightarrow 0$ and $G_i = G_j = 1$, $\{i, j\} \in \{1, 2, \ldots, M\}$, $i \neq j$, the channel capacity of the P2P link $\mathcal{C}_i \rightarrow \mathcal{C}_j$ in WiNoC can be determined by

$$C_{ij} \approx \sum_{k=1}^{K} \Delta f \left(\log_2 \frac{\varphi_{ij}}{\Phi_{ij,k}}\right)^+, \quad (14)$$

where

$$\Phi_{ij,k} = \frac{\zeta_B d_{ij}^4 \Delta f \left[T_S + (T_S + T_0)\kappa_k d_{ij}\right]}{h_i^2 h_j^2} \quad (15)$$

and φ_{ij} is chosen such that

$$\sum_{k=1}^{K} \left(\varphi_{ij} - \Phi_{ij,k}\right)^+ = P_{T,i}. \quad (16)$$

Proof: As $h_i \ll d_{ij}$, $h_j \ll d_{ij}$ and $d_{ij} \rightarrow 0$, applying Maclaurin series [33, eq. (0.318.2)], it can be approximated that

$$\sin^2\left(\frac{2\pi h_i h_j f_k \sqrt{\epsilon_r}}{c d_{ij}}\right) \approx \left(\frac{2\pi h_i h_j f_k \sqrt{\epsilon_r}}{c d_{ij}}\right)^2, \quad (17)$$

$$\prod_{g=1}^{N} \prod_{k_g=1}^{N_g} e^{\kappa_k^{(k_g,g)} d_{ij}} \approx 1 + \sum_{g=1}^{N} \sum_{k_g=1}^{N_g} \kappa_k^{(k_g,g)} d_{ij} = 1 + \kappa_k d_{ij}. \quad (18)$$

After some mathematical manipulations, we have

$$\Psi_{ij,k} \approx \Phi_{ij,k} = \frac{\zeta_B d_{ij}^4 \Delta f \left[T_S + (T_S + T_0)\kappa_k d_{ij}\right]}{h_i^2 h_j^2} \quad (19)$$

Substituting (19) into (12) with the assumption of $G_i = G_j = 1$, we obtain (14). The corollary is proved. □

Let us define $\gamma_{ij,k} \triangleq \frac{\varphi_{ij}}{\Phi_{ij,k}}$, $\{i, j\} \in \{1, 2, \ldots, M\}$, $i \neq j$, $k = 1, 2, \ldots, K$, as the signal-to-noise ratio (SNR) at the receiver core $\mathcal{C}_j$ of the link $\mathcal{C}_i \rightarrow \mathcal{C}_j$ at frequency f_k and denote the Gaussian capacity function of a point-to-point communications in WiNoC by $C(x) \triangleq \sum_{k=1}^{K} \Delta f \left(\log_2 x_k\right)^+$ for simplicity. Hereafter, C_{ij} in (14) can be expressed as $C_{ij} = C(\gamma_{ij})$.

VI. CAPACITY OF RELAY CHANNEL IN A WINOC

In this section, let us first investigate a typical relay communication between three cores in a WiNoC as shown in Fig. 2. The analysis for the general model will be investigated in Section VII. We first derive the upper bounds on the channel capacity of a typical relay channel in a single-relay WiNoC. Then, two relaying protocols, including DF and AF, will be presented followed by the introduction of a hybrid DF-AF protocol that can be considered for a multi-relay WiNoC.

[5]Note that the noise power in our proposed channel model varies as a function of both distance and frequency which is dependent on the compositions of the transmission medium within a WiNoC.

$$\Lambda_{ij,k}^2 = \frac{G_i G_j \sin^2\left(\frac{2\pi h_i h_j f_k \sqrt{\epsilon_r}}{c d_{ij}}\right)}{\zeta_B \epsilon_r \left(\frac{2\pi d_{ij} f_k}{c}\right)^2 \Delta f \left[(T_S + T_0) \prod_{g=1}^{N} \prod_{k_g=1}^{N_g} e^{\frac{\zeta_A}{\zeta_G} \frac{p^2}{p_0} \frac{T_p}{T_S^2} q^{(k_g,g)} S^{(k_g,g)} \xi^{(k_g,g)} d_{ij}} - T_0\right]}. \quad (11)$$

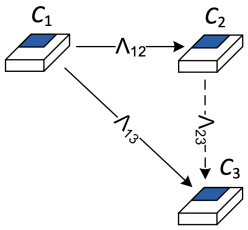

FIGURE 2. System model of a relay channel in WiNoC.

A. BOUNDS ON THE CHANNEL CAPACITY

Inspired by the concept of cooperative relay in wireless networks, the Gaussian relay channel models are adopted for the communications between three on-chip wireless cores $\mathcal{C}_1$, $\mathcal{C}_2$ and $\mathcal{C}_3$ in a WiNoC playing the roles of a source node, a relay node and a destination node, respectively. As shown in Fig. 2, in the first time slot, $\mathcal{C}_1$ broadcasts a data packet $\mathbf{x}_1$ to both $\mathcal{C}_2$ and $\mathcal{C}_3$. Then, $\mathcal{C}_2$ processes the data received from $\mathcal{C}_1$ prior to forwarding the processed data, i.e. $\mathbf{x}_2$, to $\mathcal{C}_3$ in the second time slot. The received data packets at $\mathcal{C}_2$ and $\mathcal{C}_3$ can be written by

$$\mathbf{y}_2 = \Lambda_{12}\mathbf{x}_1 + \mathbf{n}_2, \tag{20}$$

$$\mathbf{y}_3 = \Lambda_{13}\mathbf{x}_1 + \Lambda_{23}\mathbf{x}_2 + \mathbf{n}_3, \tag{21}$$

respectively, where Λ_{ij}, $\{i,j\} \in \{1,2,3\}$, $i \neq j$, denotes the channel gains of the links $\mathcal{C}_i \to \mathcal{C}_j$ given by (11). Here, $\mathbf{n}_2$ and $\mathbf{n}_3$ are independent circularly symmetric complex Gaussian noise vectors at cores $\mathcal{C}_2$ and $\mathcal{C}_3$, respectively, with each entry having zero mean and variance of 1.

It can be observed in (21) that, with cooperative diversity, the received data packet at $\mathcal{C}_3$ depends on not only the data packet transmitted from $\mathcal{C}_1$ over direct link, but also the data packet processed and forwarded from $\mathcal{C}_2$. The cooperation between two wireless on-chip cores $\mathcal{C}_1$ and $\mathcal{C}_3$ is basically limited by the bounds of broadcast phase, i.e. $\mathcal{C}_1 \to \{\mathcal{C}_2, \mathcal{C}_3\}$, and multiple access phase, i.e. $\{\mathcal{C}_1, \mathcal{C}_2\} \to \mathcal{C}_3$.

Following the same approach as in the derivation of the cutset (CS) bounds for data flow in graphical networks [34], [35, eq. (16.4)], the capacity of the Gaussian relay channels in WiNoC can be upper bounded as in (22) (see the bottom of the page), where γ_{ij}, $\{i,j\} \in \{1,2,3\}$, $i \neq j$, is the SNR of the channel $\mathcal{C}_i \to \mathcal{C}_j$ as derived in Section IV.

Additionally, it can be noticed that the capacity of relay channel is lower bounded by the capacity of the direct transmission (DT) between $\mathcal{C}_1$ and $\mathcal{C}_3$ [35, eq. (16.1)], i.e.

$$C \geq C_{DT} = C(\gamma_{13}). \tag{23}$$

With a notice that a low-complexity processing is preferable, AF and DF protocols are investigated in this work for the relay communications in WiNoC.

B. DECODE-AND-FORWARD (DF)

In DF protocol, $\mathcal{C}_2$ decodes the data from $\mathcal{C}_1$, re-encodes and forwards the data packet to $\mathcal{C}_3$ [16], [34]. It is therefore required that $\mathcal{C}_2$ decodes the whole data packet with no error and $\mathcal{C}_3$ needs to combine both the data packet received from $\mathcal{C}_1$ and the repeated data packet from $\mathcal{C}_2$. The capacity of the relay channel can be accordingly lower bounded by [35, eq. (16.6)]

$$C \geq C_{DF} = \min\{C(\gamma_{12}), C(\gamma_{13} + \gamma_{23})\}. \tag{24}$$

It can be observed in (25) that the capacity of the DF protocol depends on the location of the relay core $\mathcal{C}_2$ in relation to $\mathcal{C}_1$ and $\mathcal{C}_3$ as in the following cases:

1) *$\mathcal{C}_2$ near $\mathcal{C}_1$ having $\gamma_{12} \geq \gamma_{13} + \gamma_{23}$*:

$$C_{DF} = C(\gamma_{13} + \gamma_{23}). \tag{25}$$

2) *$\mathcal{C}_2$ near $\mathcal{C}_3$ or in the middle between $\mathcal{C}_1$ and $\mathcal{C}_3$ having $\gamma_{23} \geq \gamma_{12}$*:

$$C_{DF} = C(\gamma_{12}). \tag{26}$$

Notice that if $\mathcal{C}_2$ is very near $\mathcal{C}_3$ with $\gamma_{12} \approx \gamma_{13}$, then $C_{DF} \approx C_{DT}$ (see (23)). This means the exploitation of the relay core is not necessary in this case, and the DT is preferable achieving the same performance as in the DF scheme.

C. AMPLIFY-AND-FORWARD (AF)

In AF protocol, $\mathcal{C}_2$ simply amplifies the data packet receive from $\mathcal{C}_1$ and forwarded its amplified version to $\mathcal{C}_3$ where both versions of the packet are combined. The capacity of the AF protocol can be lower bounded by [16], [36]

$$C \geq C_{AF} = C\left(\gamma_{13} + \frac{\gamma_{12}\gamma_{23}}{\gamma_{12} + \gamma_{23} + 1}\right). \tag{27}$$

Comparing the DF and AF protocols, let us consider the following two cases as in Section VI-B, i.e.:

1) *$\mathcal{C}_2$ near $\mathcal{C}_1$*: It can be noticed that for all γ_{12}, γ_{23}, we have

$$\frac{\gamma_{12}\gamma_{23}}{\gamma_{12} + \gamma_{23} + 1} < \min\{\gamma_{12}, \gamma_{23}\}.$$

Therefore, from (25) and (27), we can deduce that $C_{AF} < C_{DF}$.

2) *$\mathcal{C}_2$ near $\mathcal{C}_3$*: From (26) and (27), we can find that $C_{AF} > C_{DF}$ when

$$\gamma_{13} + \frac{\gamma_{12}\gamma_{23}}{\gamma_{12} + \gamma_{23} + 1} > \gamma_{12}. \tag{28}$$

$$C \leq C_{CS} = \begin{cases} C\left(\dfrac{\left(\sqrt{\gamma_{12}\gamma_{23}} + \sqrt{\gamma_{13}(\gamma_{13} + \gamma_{12} - \gamma_{23})}\right)^2}{\gamma_{13} + \gamma_{12}}\right) & \text{if } \gamma_{12} \geq \gamma_{23}, \\ C(\gamma_{13} + \gamma_{12}) & \text{otherwise,} \end{cases} \tag{22}$$

Solving (28), after some mathematical manipulation, we obtain

$$\gamma_{12} < \frac{\gamma_{13} - 1 + \sqrt{(\gamma_{13}+1)^2 + 4\gamma_{13}\gamma_{23}}}{2}. \quad (29)$$

In particular, when $\mathcal{C}_2$ is located very near to $\mathcal{C}_3$, we can approximate $\gamma_{13} \approx \gamma_{12}$. Given the fact that $\gamma_{23} > \gamma_{13}$, it can be easily proved that the condition in (29) is satisfied, and thus the AF protocol is dominant to the DF protocol in this case.

3) *$\mathcal{C}_2$ in the middle between $\mathcal{C}_1$ and $\mathcal{C}_3$ with $\gamma_{12} \approx \gamma_{23}$*: With a notice that both γ_{12} and γ_{23} are much larger than 1 in short-distance communications at high frequency band, we can rewrite C_{AF} in (27) as

$$C_{AF} \approx C(\gamma_{13} + \gamma_{12}/2). \quad (30)$$

From (26) and (30), it can be easily observed that, if $\gamma_{13} < \gamma_{12}/2$, then $C_{AF} < C_{DF}$. In fact, the relay core $\mathcal{C}_2$ is practically employed to assist the communication between two cores $\mathcal{C}_1$ and $\mathcal{C}_3$ having a weak direct link with a very low SNR compared to the relaying links. The DF protocol therefore outperforms the AF in this case.

VII. PROPOSED HYBRID DF-AF (HDA) FOR MULTI-RELAY WINOC

As noted in subsections VI-B and VI-C, DF protocol is preferable to the AF when a relaying core is located either nearby a source core or in the region between the source and destination cores, while the AF protocol should be selected when the relaying core is close to the destination core. This accordingly motivates us to propose a hybrid DF-AF (HDA) protocol where the relaying core employ either DF or AF depending on its physical position with respect to the source and destination cores.

Specifically, in the HDA protocol, core $\mathcal{C}_2$ employs AF protocol when it is near core $\mathcal{C}_3$, i.e. $d_{12} > d_{23}$, otherwise $\mathcal{C}_2$ performs DF protocol if $d_{12} \leq d_{23}$. The capacity of the HDA protocol is therefore given by

$$C_{HDA} = \begin{cases} C_{DF} = C(\gamma_{13} + \gamma_{23}), & \text{if } d_{12} \leq d_{23} \\ C_{AF} = C\left(\gamma_{13} + \dfrac{\gamma_{12}\gamma_{23}}{\gamma_{12} + \gamma_{23} + 1}\right), & \text{if } d_{12} > d_{23}. \end{cases} \quad (31)$$

Considering a general model of WiNoC (see Fig. 1), the HDA can be extended for a multi-relay WiNoC consisting of a source core $\mathcal{C}_1$, multiple relaying cores $\{\mathcal{C}_2, \mathcal{C}_3, \ldots, \mathcal{C}_{M-1}\}$ and a destination core $\mathcal{C}_M$ which are assumed to be allocated as in a two-dimensional grid graph. Given the fact that relaying cores could be located at different positions between source and destination cores, the proposed HDA is employed at $\{\mathcal{C}_2, \mathcal{C}_3, \ldots, \mathcal{C}_{M-1}\}$ to assist the communication from $\mathcal{C}_1$ to $\mathcal{C}_M$.

The capacity of the HDA protocol for a relaying link $(\mathcal{C}_1 - \mathcal{C}_i - \mathcal{C}_M)$, $i = 1, 2, \ldots, M-1$, can be similarly derived as in (31), i.e.

$$C_{HDA}^{(i)} = \begin{cases} C(\gamma_{1M} + \gamma_{iM}), & \text{if } d_{1i} \leq d_{iM} \\ C\left(\gamma_{1M} + \dfrac{\gamma_{1i}\gamma_{iM}}{\gamma_{1i} + \gamma_{iM} + 1}\right), & \text{if } d_{1i} > d_{iM}, \end{cases} \quad (32)$$

where d_{ij} and γ_{ij}, $\{i, j\} \in \{1, 2, \ldots, M\}$, $i \neq j$, are the distance and SINR of the link $\mathcal{C}_i \to \mathcal{C}_j$, respectively. For convenience, let γ_{1iM} denote the received SINR of the relaying link $(\mathcal{C}_1 - \mathcal{C}_i - \mathcal{C}_M)$ using the HDA protocol, which can be written as

$$\gamma_{1iM} = \begin{cases} \gamma_{iM}, & \text{if } d_{1i} \leq d_{iM} \\ \dfrac{\gamma_{1i}\gamma_{iM}}{\gamma_{1i} + \gamma_{iM} + 1}, & \text{if } d_{1i} > d_{iM}, \end{cases} \quad (33)$$

and $C_{HDA}^{(i)}$ in (32) can be rewritten as

$$C_{HDA}^{(i)} = C(\gamma_{1M} + \gamma_{1iM}).$$

In order to exploit all signals received from different channel links, MRC is employed at $\mathcal{C}_M$. The received SINR at $\mathcal{C}_M$ taking into account direct link and all relaying links, denoted as γ_M, is thus given by

$$\gamma_M = \gamma_{1M} + \sum_{i=2}^{M-1} \gamma_{1iM}. \quad (34)$$

The capacity of the HDA protocol for multi-relay WiNoC with MRC is therefore computed by

$$C_{HDA}^{(MRC)} = C(\gamma_M) = C\left(\gamma_{1M} + \sum_{i=2}^{M-1} \gamma_{1iM}\right). \quad (35)$$

Although all relaying cores could be exploited to assist the communications between the source and destination cores, they may be busy working on other tasks and thus could not fully support such data transmission as required. Let us denote ϱ_i, $i = 2, \ldots, M-1$, as the fraction of power at the relaying core $\mathcal{C}_i$ that has been allocated for other tasks. Taking into account this practical issue, the capacity of the HDA protocol for multi-relay WiNoC can be generally written by

$$C_{HDA}^{(MRC)} = C\left(\gamma_{1M} + \sum_{i=2}^{M-1} (1 - \varrho_i)\gamma_{1iM}\right). \quad (36)$$

VIII. NUMERICAL RESULTS

In this section, we first present the numerical results for the capacity of relay channels in WiNoC with different relaying approaches along with the analysis of the impacts of transmission medium on the relay communications probably realised within a chip. The effectiveness of the proposed relay channel model taking into account both DPL and MAA is then evaluated with respect to the conventional approach where only pure air is considered with no MAA. Furthermore, the performance of the proposed HDA scheme dealing with different relay positions and its application for multi-relay WiNoC are presented to show the extendability of the proposed channel modelling. The numerical results of channel capacity

were obtained in MATLAB using the theoretically derived expressions in Section VI with relay channel modelling for WiNoC and the parameters of various gas compositions in the HITRAN database [31].

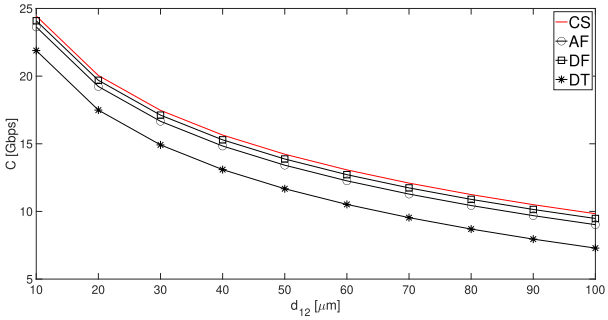

FIGURE 3. Capacity of relay channels in WiNoC versus distance between two adjacent cores $\mathcal{C}_1$ and $\mathcal{C}_2$.

A. CAPACITY OF RELAYING IN WINOC & IMPACTS OF TRANSMISSION MEDIUM ON ITS PERFORMANCE

Let us first consider a typical relay channel in WiNoC as shown in Fig. 2 consisting of three cores $\mathcal{C}_1, \mathcal{C}_2$ and $\mathcal{C}_3$. Fig. 3 plots the capacity of relaying, i.e. C in [Gbps], as a function of the distance between two adjacent cores $\mathcal{C}_1$ and $\mathcal{C}_2$, i.e. d_{12} in [μm]. The communications between two cores $\mathcal{C}_1$ and $\mathcal{C}_3$ is realised via a relay core $\mathcal{C}_2$ employing either AF or DF protocols. The bounds of the channel capacity consisting of the CS upper bound (see (22)) and the DT lower bound (see (23)) are also provided for comparison. Each core is assumed to deploy the same antenna having a height of 2 μm, i.e. $h_1 = h_2 = h_3 = 2$ μm, the ambient pressure is set as 100 kPa, the system electronic temperature is 296 K and the transmission frequency is 60 GHz. The other distances between cores are set as $d_{23} = d_{12}$ and $d_{13} = d_{12}\sqrt{2}$. Given a transmission bandwidth of 1 GHz, the power for sub-bands is allocated by water-filling method for the DT protocol as in Proposition 1, while equal power allocation is employed for both relaying protocols. It can be observed in Fig. 3 that the DF scheme achieves a higher capacity than the AF scheme, while both schemes are bounded by the DT and CS bounds. This accordingly verifies the statement in Section VI-C regarding the better performance achieved with the DF scheme when the relay core is in the middle between the source and destination cores.

The impacts of system electronic temperature, i.e. T_S, and ambient pressure, i.e. p, on the performance of relaying in WiNoC are illustrated in Figs. 4 and 5, respectively. In Fig. 4, the channel capacity, i.e. C in Gbps, is plotted as a function of T_S given $p = 100$ kPa, while C is plotted against p in Fig. 5 given $T_S = 296$ K. The other parameters are similarly set as in Fig. 3, while the distance between $\mathcal{C}_1$ and $\mathcal{C}_2$ is fixed as $d_{12} = 100\mu$m. It can be observed in both figures that the increase of either the temperature or the pressure causes the degradation of the performance of the relaying in the WiNoC. This is indeed caused by the increased path loss due to the MAA as claimed in Remarks 2 and 3 on the

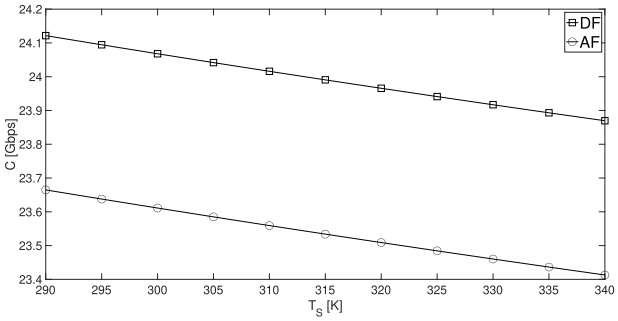

FIGURE 4. Capacity of relay channels in WiNoC versus system electronic noise temperature.

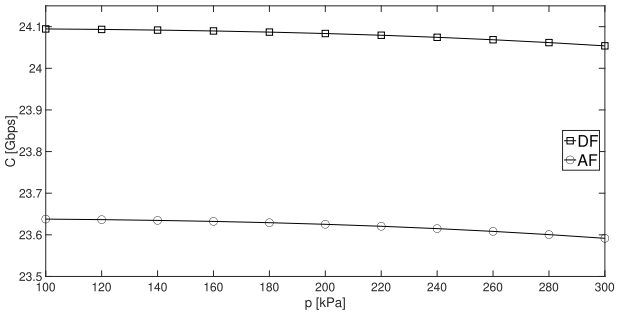

FIGURE 5. Capacity of relay channels in WiNoC versus ambient pressure.

environmental awareness of the proposed channel model. Additionally, the DF protocol is shown to achieve a better performance than the AF protocol for all scenarios of the environment, which can be similarly perceived as in Fig. 3.

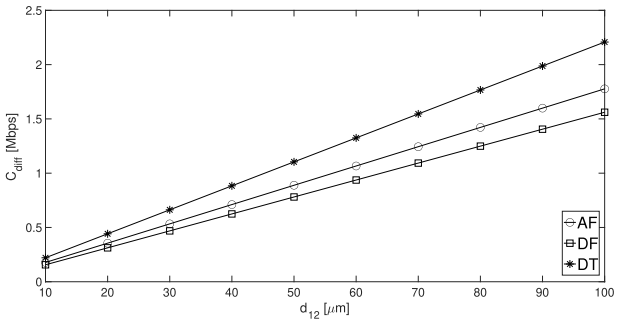

FIGURE 6. Capacity difference of different channel models for relay communications in WiNoC with/without MAA.

B. COMPARISON OF RELAY CHANNEL MODELS IN WINOC

Evaluating the effectiveness of the proposed channel model, Figs. 6, 7 and 8 sequentially plot the capacity difference between the proposed channel model and the conventional channel model, i.e. $C_{\text{diff}} \triangleq C^{(\text{with no MAA})} - C^{(\text{with MAA})}$,[6] as a function of the distance between two adjacent cores $\mathcal{C}_1$ and $\mathcal{C}_2$, i.e. d_{12} in μm, with respect to different relaying schemes, system electronic noise temperature, i.e. T_S, and ambient pressure, i.e. p, respectively. Specifically, in Fig. 6, C_{diff} is plotted for AF, DF and DT schemes; three scenarios

[6]Note that $C^{(\text{with MAA})}$ is derived as in Section VI with different relaying schemes, while $C^{(\text{with no MAA})}$ can be similarly derived when there is only DPL, i.e. $L^{(d)}$, constituted in the total path loss.

of $T_S = \{290, 310, 340\}$ K are considered in Fig. 7; and $p = \{100, 200, 300\}$ kPa in Fig. 8. As shown in Fig. 6, C_{diff} of the AF and DF protocols is smaller when compared to the DT, which accordingly reflects the effectiveness of the relaying protocols in reducing the performance loss. For instance, the DF and AF protocols are shown to have a lower performance loss of 0.7 Mbps and 0.5 Mbps, respectively, than the DT protocol when $d_{12} = 100\ \mu$m. It can be observed in all three figures that the capacity difference increases as the distance between cores increases. This means that a much higher performance loss is caused by the MAA over the distance. Also, such increase of C_{diff} varies with respect to the system electronic temperature and ambient pressure as illustrated in Figs. 7 and 8, respectively. These observations reconfirm the statements in Remarks 2 and 3 concerning the effects of the environment on the channel modelling.

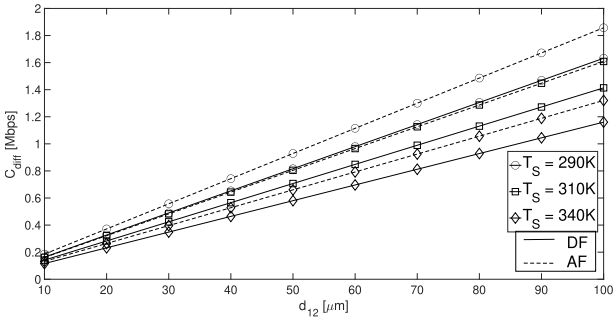

FIGURE 7. Capacity difference of different relaying channel models in WiNoC w.r.t. system electronic noise temperature.

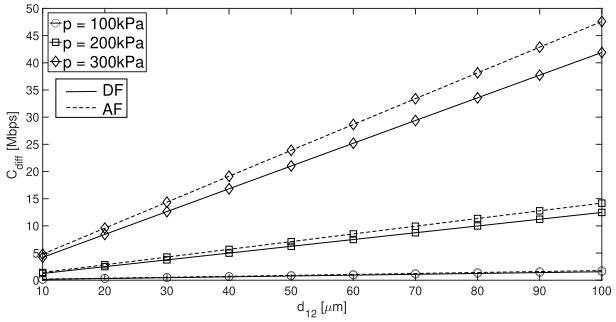

FIGURE 8. Capacity difference of different relaying channel models in WiNoC w.r.t. ambient pressure.

C. PERFORMANCE OF THE PROPOSED HDA SCHEME AND MULTI-RELAY WINOC

Considering a general model of WiNoC where the relaying core can be at different positions between the source and destination cores, Fig. 9 plots the capacity of relay channel as a function of the distance between cores $\mathcal{C}_2$ and $\mathcal{C}_3$, i.e. d_{23}, with reference to different relaying protocols including AF, DF and the proposed HDA. Two scenarios of propagation environment are considered, including i) $T_S = 290$K, $p = 100$kPa and ii) $T_S = 330$K, $p = 200$kPa. Other distances between cores are set as $d_{12} = 10\ \mu$m and $d_{13} = \sqrt{d_{12}^2 + d_{23}^2}$, while other simulation parameters are similarly set as in Fig. 3. It can be observed in Fig. 9 that the DF

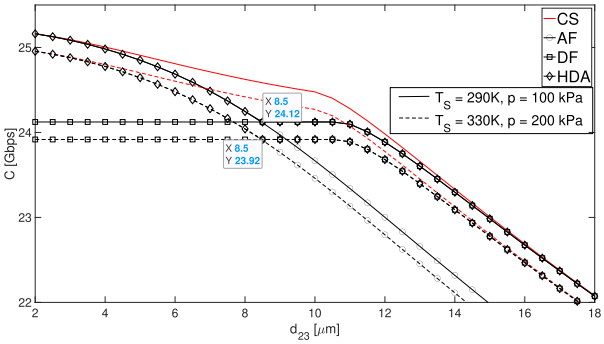

FIGURE 9. Capacity of relay channel in WiNoC versus unequal distance between cores $\mathcal{C}_2$ and $\mathcal{C}_3$ w.r.t. propagation environment.

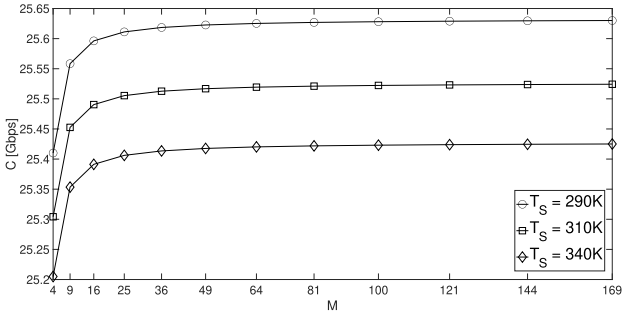

FIGURE 10. Capacity of relay channel in WiNoC versus number of cores.

protocol achieves a higher capacity than the AF protocol when $d_{23} \geq 8.5\ \mu$m, while the AF outperforms the DF protocol when $d_{23} < 8.5\ \mu$m. This is in fact discussed in Section VI-C showing the performance comparison of the AF and DF protocols related to the location of the cores. Additionally, the proposed HDA protocol is shown to achieve the best performance over both the AF and DF protocols, and thus, as stated in Section VII, can be regarded as an adaptive approach to cope with the unbalanced distance between the relaying core and the two end cores.

Furthermore, it can be observed in Fig. 9 that the capacity achieved in the first case is higher than that in the second case for all relaying protocols. However, the crossing points of AF and DF protocols in both cases are obtained at the same distance between the cores, i.e. when $d_{23} = 8.5\mu$m. This reflects the fact that the distance between the cores should be considered in the HDA protocol as derived in (31), while the system electronic temperature and ambient pressure nevertheless only have impacts on the performance of the relaying protocols as illustrated in Figs. 4 and 5, respectively.

Extending to a general WiNoC with variant number of cores, Fig. 10 plots the channel capacity as a function of the number of cores, i.e. M, at different operating temperature, i.e. T_S. The cores are assumed to located in a two-dimensional grid having the same distance, i.e. $d = 10\ \mu$m, between two adjacent cores in both horizontal and vertical axes. Here, the source and destination cores are located at the bottom-left and top-right corners, respectively, within the chip. Three scenarios of $T_S = \{290, 310, 340\}$ K are considered and other parameters are set as in Fig. 9. It can be observed in Fig. 10 an increased number of cores results in a higher capacity,

especially when the number of cores increases from 4 to 36 cores. Additionally, with a large number of cores deployed on a large chip, we can still achieve the same performance as in a small chip even though the distance between the source and destination cores will get longer. Indeed, with more intermediate cores, the communication between the source and the destination cores is assisted by various relaying links besides the direct link. This intuitive observation can also be verified by (35) in Section VI with MRC approach employed at the destination cores to combine the data received from direct link and all relaying links.

IX. CONCLUSION

In this article, we have proposed a relay communication channel for the communications between the far-end wireless cores in WiNoCs. Considering high frequency band, dielectric material and gas compositions of the transmission medium within the chip package are taken into account in the developed channel model, based on which the channel capacity has been derived for the relay channel in a typical single-relay WiNoC employing DF and AF relaying protocols. In particular, a HDA relaying protocol has been proposed to maximise the performance of both the DF and AF protocols with respect to the location of the wireless cores. It has been shown that the HDA protocol achieves the best performance close to the cutset bound of the relay channel over the whole range of the location of the intermediate core between two end cores. Furthermore, the proposed HDA protocol has been extended for a multi-relay WiNoC where intermediate cores are exploited to assist the communications via different relay links. The employment of a large number of cores on a large chip as the relays has shown to enhance the performance of the communications between the two far-end cores as if they were located close to each other on a small chip. The future work would be the investigation of resource allocation for the relaying protocols in the WiNoCs.

APPENDIX A PROOF OF THEOREM 1

The total noise temperature T_{tot} [K], of the P2P channel in a WiNoC consists of system electronic noise temperature T_S [K], molecular absorption noise temperature T_M [K] and other noise source temperature, T' [K], i.e.

$$T_{tot} = T_S + T_M + T'. \tag{37}$$

Notice that $T' \ll T_S + T_M$, and thus it can be approximated that

$$T_{tot} \approx T_S + T_M. \tag{38}$$

Here, T_M depends on the transmittance of the medium τ_{ij}, which can be given by

$$T_M = T_0(1 - \tau_{ij}), \tag{39}$$

where τ_{ij} is given by (3). From (3) and (4), T_M can be derived as

$$T_M = T_0 \left(1 - \prod_{g=1}^{N} \prod_{k_g=1}^{N_g} e^{\frac{\zeta_A}{\zeta_G} \frac{p^2}{p_0} \frac{T_p}{T_S^2} q^{(k_g,g)} S^{(k_g,g)} \xi^{(k_g,g)} d_{ij}}\right). \tag{40}$$

Substituting (40) into (38), we obtain

$$T_{tot} \approx T_S + T_0 \left(1 - \prod_{g=1}^{N} \prod_{k_g=1}^{N_g} e^{\frac{\zeta_A}{\zeta_G} \frac{p^2}{p_0} \frac{T_p}{T_S^2} q^{(k_g,g)} S^{(k_g,g)} \xi^{(k_g,g)} d_{ij}}\right). \tag{41}$$

The total noise power at $\mathcal{C}_j$ is therefore given by

$$P_N = \zeta_B \int_B T_{tot} df. \tag{42}$$

Dealing with the frequency-selective channel within the WiNoC, the channel bandwidth B can be divided into K narrow sub-bands, i.e. $\Delta f = B/K$, each of which is allocated a power of P_{T,i_k}. Given the transmission power constraint at $\mathcal{C}_i$, i.e. $\sum_{k=1}^{K} P_{T,i_k} \leq P_{T,i}$, the channel capacity of the P2P channel can be expressed by

$$C = \max_{\substack{P_{T,i_1}, P_{T,i_2}, \ldots, P_{T,i_K} \\ \sum_{k=1}^{K} P_{T,i_k} \leq P_{T,i}}} \sum_{k=1}^{K} \Delta f \log_2 \left(1 + \frac{P_{T,i_k}}{\zeta_B L_{ij,k} T_{tot,k} \Delta f}\right), \tag{43}$$

where $L_{ij,k}$ is the total attenuation and $T_{tot,k}$ is the total noise temperature at f_k.

Let us denote the channel gain by $\Lambda_{ij,k}$ having

$$\Lambda_{ij,k}^2 = \frac{1}{\zeta_B L_{ij,k} T_{tot,k} \Delta f}. \tag{44}$$

Substituting (9) and (41) into (44), $\Lambda_{ij,k}^2$ can be determined by (45) (see the top of next page). Accordingly, (43) can be rewritten as (10). The theorem is proved.

APPENDIX B PROOF OF PROPOSITION 1

Consider a point-to-point communication link $\mathcal{C}_i \rightarrow \mathcal{C}_j$, $\{i, j\} \in \{1, 2, 3\}$, $i \neq j$. Let λ_{ij} be the Lagrange multiplier associated with the power constraint $\sum_{k=1}^{K} P_{T,i_k} - P_{T,i} = 0$, the Lagrangian of (10) can be formed as

$$\mathcal{L}(\lambda_{ij}, P_{T,i_k}) = \sum_{k=1}^{K} \Delta f \log_2 \left(1 + P_{T,i_k} \Lambda_{ij,k}^2\right) - \lambda_{ij} \left(\sum_{k=1}^{K} P_{T,i_k} - P_{T,i}\right). \tag{46}$$

By defining $\Psi_{ij,k}$ as in (47) (see the top of next page), we can rewrite (46) as

$$\mathcal{L}(\lambda_{ij}, P_{T,i_k}) = \sum_{k=1}^{K} \Delta f \log_2 \left(1 + \frac{P_{T,i_k}}{\Psi_{ij,k}}\right) - \lambda_{ij} \left(\sum_{k=1}^{K} P_{T,i_k} - P_{T,i}\right). \tag{48}$$

Differentiating $\mathcal{L}(\lambda_{ij}, P_{T,i_k})$ with respect to P_{T,i_k}, we have

$$\frac{\partial \mathcal{L}(\lambda_{ij}, P_{T,i_k})}{\partial P_{T,i_k}} = \frac{\Delta f}{\ln 2} \frac{1}{P_{T,i_k} + \Psi_{ij,k}} - \lambda_{ij}. \tag{49}$$

$$\Lambda_{ij,k}^2 = \frac{G_i G_j \sin^2\left(\frac{2\pi h_i h_j f_k \sqrt{\epsilon_r}}{c d_{ij}}\right)}{\zeta_B \epsilon_r \left(\frac{2\pi d_{ij} f_k}{c}\right)^2 \Delta f \left[(T_S + T_0)\prod_{g=1}^{N}\prod_{k_g=1}^{N_g} e^{\frac{\zeta_A}{\zeta_G}\frac{p^2}{p_0}\frac{T_p}{T_S^2} q^{(k_g,g)} S^{(k_g,g)} \xi^{(k_g,g)} d_{ij}} - T_0\right]}. \tag{45}$$

$$\begin{aligned}\Psi_{ij,k} &\triangleq \frac{1}{\Lambda_{ij,k}^2} \\ &= \frac{\zeta_B \epsilon_r}{G_i G_j}\left(\frac{2\pi d_{ij} f_k}{c}\right)^2 \Delta f \csc^2\left(\frac{2\pi h_i h_j f_k \sqrt{\epsilon_r}}{c d_{ij}}\right)\left[(T_S + T_0)\prod_{g=1}^{N}\prod_{k_g=1}^{N_g} e^{\frac{\zeta_A}{\zeta_G}\frac{p^2}{p_0}\frac{T_p}{T_S^2} q^{(k_g,g)} S^{(k_g,g)} \xi^{(k_g,g)} d_{ij}} - T_0\right],\end{aligned} \tag{47}$$

Solving $\frac{\partial \mathcal{L}(\lambda_{ij}, P_{T,i_k})}{\partial P_{T,i_k}} = 0$, we obtain

$$P_{T,i_k} = \frac{\Delta f}{\lambda_{ij} \ln 2} - \Psi_{ij,k} = \vartheta_{ij} - \Psi_{ij,k}, \tag{50}$$

where $\vartheta_{ij} \triangleq \Delta f / (\lambda_{ij} \ln 2)$.

Since $P_{T,i_k} \geq 0$, the solution in (50) is thus $P_{T,i_k} = (\vartheta_{ij} - \Psi_{ij,k})^+$, where $(x)^+ \triangleq \max\{0, x\}$ and ϑ can be solved using water-filling method as

$$\sum_{k=1}^{K} \left(\vartheta_{ij} - \Psi_{ij,k}\right)^+ = P_{T,i}. \tag{51}$$

This completes the proof.

REFERENCES

[1] L. Wang, X. Wang, and Y. Wang, "An approximate bufferless network-on-chip," *IEEE Access*, vol. 7, pp. 141516–141532, 2019.
[2] R. Radhika, N. Anusha, and R. Manimegalai, "A comprehensive survey on strategies in multicore architectures, design considerations and challenges," in *Proc. Int. Conf. Artif. Intell., Smart Grid Smart City Appl.*, 2019, pp. 811–818.
[3] S. Abadal, C. Han, and J. M. Jornet, "Wave propagation and channel modeling in chip-scale wireless communications: A survey from millimeter-wave to terahertz and optics," *IEEE Access*, vol. 8, pp. 278–293, 2020.
[4] A. Shacham, K. Bergman, and L. P. Carloni, "Photonic networks-on-chip for future generations of chip multiprocessors," *IEEE Trans. Comput.*, vol. 57, no. 9, pp. 1246–1260, Sep. 2008.
[5] Y. Xu and S. Pasricha, "Silicon nanophotonics for future multicore architectures: Opportunities and challenges," *IEEE Des. Test. Comput.*, vol. 31, no. 5, pp. 9–17, Oct. 2014.
[6] N. Ashokkumar, P. Nagarajan, and P. Venkatramana, "3D (dimensional)—Wired and wireless network-on-chip (NoC)," in *Inventive Communication and Computational Technologies* (Lecture Notes in Networks and Systems), vol. 89. Singapore: Springer, 2020, pp. 113–119.
[7] M. O. Agyeman and W. Zong, "An efficient 2D router architecture for extending the performance of inhomogeneous 3D NoC-based multi-core architectures," in *Proc. Int. Symp. Comput. Archit. High Perform. Comput. Workshops (SBAC-PADW)*, Oct. 2016, pp. 79–84.
[8] M. O. Agyeman, A. Ahmadinia, and N. Bagherzadeh, "Performance and energy aware inhomogeneous 3D networks-on-chip architecture generation," *IEEE Trans. Parallel Distrib. Syst.*, vol. 27, no. 6, pp. 1756–1769, Jun. 2016.
[9] S. Deb, A. Ganguly, P. P. Pande, B. Belzer, and D. Heo, "Wireless NoC as interconnection backbone for multicore chips: Promises and challenges," *IEEE J. Emerg. Sel. Topics Circuits Syst.*, vol. 2, no. 2, pp. 228–239, Jun. 2012.
[10] D. Matolak, A. Kodi, S. Kaya, D. Ditomaso, S. Laha, and W. Rayess, "Wireless networks-on-chips: Architecture, wireless channel, and devices," *IEEE Wireless Commun.*, vol. 19, no. 5, pp. 58–65, Oct. 2012.
[11] S. Abadal, A. Mestres, M. Iannazzo, J. Sole-Pareta, E. Alarcon, and A. Cabellos-Aparicio, "Evaluating the feasibility of wireless networks-on-chip enabled by graphene," in *Proc. NoCArc*, Cambridge, U.K., Dec. 2014, pp. 51–56.
[12] M. O. Agyeman, Q.-T. Vien, A. Ahmadinia, A. Yakovlev, K.-F. Tong, and T. Mak, "A resilient 2-D waveguide communication fabric for hybrid wired-wireless NoC design," *IEEE Trans. Parallel Distrib. Syst.*, vol. 28, no. 2, pp. 359–373, Feb. 2017.
[13] M. O. Agyeman, Q.-T. Vien, and T. Mak, "An analytical channel model for emerging wireless networks-on-chip," in *Proc. IEEE Int. Conf. Comput. Sci. Eng. (CSE) IEEE Int. Conf. Embedded Ubiquitous Comput. (EUC), 15th Int. Symp. Distrib. Comput. Appl. Bus. Eng. (DCABES)*, Aug. 2016, pp. 9–15.
[14] Q.-T. Vien, M. O. Agyeman, T. A. Le, and T. Mak, "On the nanocommunications at THz band in graphene-enabled wireless network-on-chip," *Math. Problems Eng.*, vol. 2017, pp. 1–13, 2017.
[15] D. W. Matolak, S. Kaya, and A. Kodi, "Channel modeling for wireless networks-on-chips," *IEEE Commun. Mag.*, vol. 51, no. 6, pp. 180–186, Jun. 2013.
[16] J. N. Laneman, D. N. C. Tse, and G. W. Wornell, "Cooperative diversity in wireless networks: Efficient protocols and outage behavior," *IEEE Trans. Inf. Theory*, vol. 50, no. 12, pp. 3062–3080, Dec. 2004.
[17] A. Sendonaris, E. Erkip, and B. Aazhang, "User cooperation diversity—Part I. System description," *IEEE Trans. Commun.*, vol. 51, no. 11, pp. 1927–1938, Nov. 2003.
[18] A. K. Biswas, N. Chatterjee, H. Mondal, G. Gogniat, and J.-P. Diguet, "Attacks toward wireless network-on-chip and countermeasures," *IEEE Trans. Emerg. Topics Comput.*, early access, Feb. 17, 2020, doi: 10.1109/TETC.2020.2973427.
[19] D. Zhao, Y. Ouyang, Q. Wang, and H. Liang, "Cm^{3}WiNoCs: Congestion-aware millimeter-wave multichannel wireless networks-on-chip," *IEEE Access*, vol. 8, pp. 24098–24107, 2020.
[20] J. Baylon, X. Yu, S. Gopal, R. Molavi, S. Mirabbasi, P. P. Pande, and D. Heo, "A 16-Gb/s low-power inductorless wideband gain-boosted baseband amplifier with skewed differential topology for wireless network-on-chip," *IEEE Trans. Very Large Scale Integr. (VLSI) Syst.*, vol. 26, no. 11, pp. 2406–2418, Nov. 2018.
[21] A. Karkar, T. Mak, N. Dahir, R. Al-Dujaily, K.-F. Tong, and A. Yakovlev, "Network-on-chip multicast architectures using hybrid wire and surface-wave interconnects," *IEEE Trans. Emerg. Topics Comput.*, vol. 6, no. 3, pp. 357–369, Jul. 2018.
[22] Y. Chen and C. Han, "Channel modeling and characterization for wireless networks-on-chip communications in the millimeter wave and terahertz bands," *IEEE Trans. Mol., Biol. Multi-Scale Commun.*, vol. 5, no. 1, pp. 30–43, Oct. 2019.
[23] A. Vashist, A. Keats, S. M. P. Dinakarrao, and A. Ganguly, "Securing a wireless network-on-chip against jamming based denial-of-service attacks," in *Proc. IEEE Comput. Soc. Annu. Symp. VLSI (ISVLSI)*, Jul. 2019, pp. 320–325.
[24] S.-B. Lee, S.-W. Tam, I. Pefkianakis, S. Lu, M. F. Chang, C. Guo, G. Reinman, C. Peng, M. Naik, L. Zhang, and J. Cong, "A scalable micro wireless interconnect structure for CMPS," in *Proc. 15th Annu. Int. Conf. Mobile Comput. Netw.*, 2009, p. 217–228.

[25] V. Vijayakumaran, M. P. Yuvaraj, N. Mansoor, N. Nerurkar, A. Ganguly, and A. Kwasinski, "CDMA enabled wireless network-on-chip," *J. Emerg. Technol. Comput. Syst.*, vol. 10, no. 4, pp. 28:1–28:20, 2014.
[26] T. Ng and W. Yu, "Joint optimization of relay strategies and resource allocations in cooperative cellular networks," *IEEE J. Sel. Areas Commun.*, vol. 25, no. 2, pp. 328–339, Feb. 2007.
[27] M. O. Hasna and M.-S. Alouini, "Optimal power allocation for relayed transmissions over Rayleigh-fading channels," *IEEE Trans. Wireless Commun.*, vol. 3, no. 6, pp. 1999–2004, Nov. 2004.
[28] D. M. Pozar, *Microwave Engineering*, 4th ed. Hoboken, NJ, USA: Wiley, 2012.
[29] T. Rappaport, *Wireless Communications: Principles and Practice*. Upper Saddle River, NJ, USA: Prentice-Hall, 2001.
[30] P. R. Gray, P. J. Hurst, S. H. Lewis, and R. G. Meyer, *Analysis and Design of Analog Integrated Circuits*, 5th ed. Hoboken, NJ, USA: Wiley, 2009.
[31] L. S. Rothman *et al.*, "The HITRAN2012 molecular spectroscopic database," *J. Quant. Spectrosc. Radiat. Transf.*, vol. 130, pp. 4–50, Nov. 2013.
[32] R. M. Goody and Y. L. Yung, *Atmospheric Radiation: Theoretical Basis*, 2nd ed. London, U.K.: Oxford Univ. Press, 1989.
[33] I. S. Gradshteyn and I. M. Ryzhik, *Table of Integrals, Series, and Products*. New York, NY, USA: Academic, 2007.
[34] T. Cover and A. E. Gamal, "Capacity theorems for the relay channel," *IEEE Trans. Inf. Theory*, vol. IT-25, no. 5, pp. 572–584, Sep. 1979.
[35] A. E. Gamal and Y.-H. Kim, *Network Information Theory*. New York, NY, USA: Cambridge Univ. Press, 2012.
[36] B. Schein and R. Gallager, "The Gaussian parallel relay network," in *Proc. IEEE ISIT*, Sorrento, Italy, Jun. 2000, p. 22.

QUOC-TUAN VIEN (Senior Member, IEEE) received the Ph.D. degree in telecommunications from Glasgow Caledonian University, U.K., in 2012. He is currently a Senior Lecturer with the Faculty of Science and Technology, Middlesex University, U.K. He has authored a textbook, co-authored five book chapters, and more than 90 research articles in ISI journals and major conference proceedings. His current research interests include physical-layer security, network coding, non-orthogonal multiple access, RF energy harvesting, device-to-device communications, heterogeneous networks, network-on-chip and the Internet of Things. He is a TPC member of the IEEE conferences. He was a recipient of the Best Paper Award from the IEEE/IFIP 14th International Conference on Embedded and Ubiquitous Computing, in 2016. He was honored as an Exemplary Reviewer of the IEEE Communications Letters, in 2017. He served as the Program Co-Chair for the INISCOM from 2018 to 2020 and the Technical Symposium Co-Chair for the SigTelCom from 2017 to 2020. He is also a frequent reviewer of the IEEE journals. He currently serves as an Editor for the *Wireless Communications and Mobile Computing* and the *International Journal of Digital Multimedia Broadcasting* and a Guest Editor for the *EAI Endorsed Transactions on Industrial Networks and Intelligent Systems*.

MICHAEL OPOKU AGYEMAN (Senior Member, IEEE) received the Ph.D. degree from Glasgow Caledonian University, U.K. He was with the Intel Embedded System Research Group, The Chinese University of Hong Kong, as a Research Fellow. He is currently an Associate Professor with the Department of Computing, University of Northampton, U.K., where he is also the Postgraduate Research Program Lead with the Faculty of Arts, Science and Technology. He has authored four books, two book chapters, and over 70 publications in major journals and conference proceedings. His main research interest is in high-performance computing and embedded systems, such as VLSI SoC design, computer architecture, reconfigurable computing, wired and wireless NoCs, smart rehabilitation solutions, embedded systems, and the Internet-of-Things. He is a Chartered Engineer and a Chartered Manager. He is a Technical Committee Member of several conferences, such as the IEEE ICCSN, IEEE ICBDA, and IEEE ICCT. He has received two Best Paper Awards from the IEEE/IFIP EUC 2016 and the Euromicro DSD 2016 for his work on wireless NoC. He was also a recipient of the 2018 International Changemaker of the Year Award in the first U.K. Ashoka U Changemenker Campus. He has been a Guest Editor of the *EAI Endorsed Transactions on Industrial Networks and Intelligent Systems*. He serves as a Reviewer of several conferences and journals, including IEEE Access.

MALLIK TATIPAMULA (Senior Member, IEEE) He is currently the CTO of Ericsson Silicon Valley, where he leads the evolution of Ericsson's technology and champion the company's next phase of innovation and growth. He held several leadership positions at F5 networks, Juniper networks, Cisco, Motorola, Nortel, and IIT Madras, Chennai, India. During 30 years of his professional career, he has played a very unique leadership role in delivering industry's most powerful innovations, standards contributions, products/solutions, and design implementation of early real-world deployments working with telecom operators, and also innovating for the future, working with academia, by anticipating what might happen next, to accelerate the architectural transitions in the telecom industry. He has identified strategic opportunities and implemented programs that have brought world-leading innovations to the telecom sector with a multi-billion dollars impact, launching over 50 products/solutions that are deployed in global telecom networks to enable these major network transitions from 2G to 5G.

He received the bachelor's degree in electronics and communications engineering from NIT, Warangal, India, the master's degree in communication systems from IIT Madras and the Ph.D. degree in information and communications engineering from The University of Tokyo, Japan. Since 2011, he has been a Visiting Professor with the King's College London. He is a Fellow of Canadian Academy of Engineering and the Institution of Engineering and Technology (IET), U.K. He received the University of California, Berkeley's Garwood Center for Corporate Innovation Award, the Technologist of the year award (sponsored by NTT) from the World Communications Awards, the IEEE Communications Society Distinguished Industry Leader Award, and the IET Achievement Medal in telecommunications. He served on several advisory boards, including Global Semiconductor Alliance, Gartner/Evanta CIO Council, Digital India Initiative, the London Digital Twin Research Center, the Chair for the Industry Advisory Board with the Garwood Center for Corporate Innovation, and an Advisor with the Center for Growth Markets at University of California at Berkeley (UC Berkeley), Berkeley. He delivered lectures and taught courses at UC Berkeley, The University of Tokyo, Stanford University, and other universities. He mentored over 100 undergrad/graduate students, delivered over 400 keynote/invited talks/tutorials/lectures, co-authored two books, over 100 publications/patents. He served on over 40 IEEE conferences committees. He has been involved in developing industry-academia partnerships in Canada, USA, U.K., and India for future technology innovations.

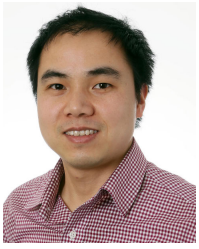

HUAN X. NGUYEN (Senior Member, IEEE) received the Ph.D. degree from the University of New South Wales, Australia, in 2007. He is currently a Professor in digital communication engineering with Middlesex University, London, U.K., where he is also the Director of the London Digital Twin Research Centre and the Head of the 5G and IoT Research Group. He leads research activities in 5G systems, machine-type communication, digital transformation, and machine learning within his university with a focus on applications in digital twins, Industry 4.0, and critical applications, such as disasters, smart manufacturing, intelligent transportation, and e-health. He has been leading major council/industry funded projects. He has been serving as the Chair for international conferences, such as ATC'15, IWNPD'17, FoNeS-IoT'20, PIMRC'20, and ICT'19-'20-'21.